

Title	Formal quantum efficiencies for the photocatalytic reduction of CO ₂ in a gas phase batch reactor
Authors	Cortes, Maria Ana L. R. M.;Hamilton, J. W. J.;Sharma, P. K.;Brown, A.;Nolan, Michael;Gray, K. A.;Byrne, J. Anthony
Publication date	2018-10-23
Original Citation	Cortes, M. A. L. R. M., Hamilton, J. W. J., Sharma, P. K., Brown, A., Nolan, M., Gray, K. A. and Byrne, J. A. (2018) 'Formal quantum efficiencies for the photocatalytic reduction of CO ₂ in a gas phase batch reactor', Catalysis Today. doi:10.1016/j.cattod.2018.10.047
Type of publication	Article (peer-reviewed)
Link to publisher's version	10.1016/j.cattod.2018.10.047
Rights	© 2018, Elsevier B.V. All rights reserved. This manuscript version is made available under the CC-BY-NC-ND 4.0 license. - https://creativecommons.org/licenses/by-nc-nd/4.0/
Download date	2023-05-05 02:53:01
Item downloaded from	http://hdl.handle.net/10468/7148

Title: Formal Quantum Efficiencies for the Photocatalytic Reduction of CO₂ in a Gas Phase Batch Reactor

Authors: M.A.L.R.M. Cortes^{*a}, J.W.J. Hamilton^a, P.K. Sharma^a, A. Brown^a, M. Nolan^b, K.A. Gray^c, J.A. Byrne^a.

^aNIBEC, Ulster University, Newtownabbey, BT37 0QB, UK

^bTyndall National Institute, University College Cork, Lee Maltings, Cork, Ireland

^cNorthwestern University, 2145 Sheridan Road, Evanston, IL 60208, USA

*Corresponding author: Cortes-MA@ulster.ac.uk

Abstract

The photocatalytic reduction of CO₂ to fuels, or useful products, is an area of active research. In this work, nanoengineering and surface modification of titania were investigated as approaches for improving the CO₂ reduction efficiency in a fixed-bed gas phase batch photoreactor under UV-Vis irradiation. Titania nanotubes were prepared by a hydrothermal method, and TiO₂ (P25) was surface modified with copper clusters. Unmodified TiO₂ (P25) was used as the bench-mark comparison. The titania nanotubes and Cu-TiO₂ materials showed higher efficiency for the photocatalytic reduction of CO₂ to yield CH₄ as compared to P25. Carbon monoxide yields were similar for all photocatalysts tested. The photocatalytic reduction of CO₂ was observed on all photocatalyst tested, with the nanotubes proving to be the most efficient for the production of CH₄. The product yields per mass of catalyst observed in this work are similar to those reported in the literature (with similar reactor parameters) but the calculated formal quantum efficiencies for CO₂ reduction are very low (4.41×10^{-5} to 5.95×10^{-4}).

Keywords: CO₂ photoreduction, titanium dioxide, GC-MS controls, mechanism, quantum efficiency

Research highlights

Hydrothermal titania nanotubes, Cu modified TiO₂ and TiO₂ P25 tested for the photocatalytic reduction of CO₂ in a batch gas phase photoreactor

CH₄ and CO were observed as the main products of photocatalytic reduction of CO₂

CO₂ reduction efficiencies in terms of product yield per gram of catalyst correlate to the literature

Formal quantum efficiencies for CO₂ reduction are low.

Titania nanotubes give much better yield for CH₄ as compared to Cu-TiO₂ and P25

1. Introduction/ background

Global warming and climate change are of major concern to humanity and the environment, with CO₂ being the predominant greenhouse gas responsible for global warming. In order to reduce the levels CO₂ emitted to the atmosphere, one can employ capture and utilisation, and artificial photosynthesis is a potential route to converting CO₂ to fuels or useful chemicals. The photo-driven reduction of CO₂ into fuels and/or platform chemicals has been reported using heterogeneous photocatalysis with a range of different photocatalytic materials and different reactor geometries and conditions which affect observed product distributions [1, 2]. CO₂ photoreduction products including CH₄, CH₃OH, CO, small organic acids and, occasionally some higher carbon products, have all been reported for photocatalytic CO₂ reduction [3].

The ability to control the product distribution and yield from photocatalytic CO₂ reduction systems is a research target. Some platform chemicals e.g. CO, HCOOH etc. are more valuable than solar fuels e.g. CH₄, CH₃OH, and may represent a better product targets for synthesis [4]. To switch product distribution towards a desired product, reaction conditions are controlled to limit undesirable reactions or promote a reaction leading to a desired product [5].

Titanium dioxide (TiO₂) is the most commonly used research photocatalyst due to its comparatively good photocatalytic activity. Since TiO₂ has a low solar efficiency due to its wide band gap requiring UV excitation, metal modification of the parent titania has been studied as a means to achieving the photocatalytic reduction of CO₂ [1, 6]. The presence of carbonaceous surface species was found by some groups to complicate the results of isotopic ¹³C CO₂ photoreduction studies, the rationale being that if ¹³C labelled CO₂ was the used, ¹³C products would confirm the CO₂ as the source of photocatalytic products. Considering the literature, using a range of photocatalytic materials, some studies showed mixed products [7-13], with only a few reporting solely ¹³C products [14-17]. The observation of ¹²C products in isotope studies are often assumed to be from surface contaminants, resulting in some authors questioning if the products and yields reported in other photoreduction studies, were due to contaminant oxidation, rather than true CO₂ conversion [7, 18]. Studies from a range of laboratories have used ¹³CO₂ to confirm CO₂ as the source of methane, methanol, CO etc. produced by photocatalysis [9, 12, 14]. Given the potential for differing kinetics with isotopically labelled samples and the complexity/availability of GC-MS, it has been recommended that researchers utilise a control run in the absence of CO₂ instead of isotopically labelled ¹³C as evidence against photo-Kolbe / side reactions as the source of CO₂ reduction products [19, 20]. However, efforts to eliminate CO₂ prior to photoreduction experiments can be far from trivial due to pre-adsorption on catalyst surfaces [21] and unwanted traces of CO₂ dissolved in liquid water.

There is some difficulty in comparing results of photocatalytic CO₂ reduction studies reported due to variations in reactors and parameters. CO₂ reduction yields are usually reported in $\mu\text{mol h}^{-1} \text{g}^{-1}$ of catalyst, however, this normalisation to per gram of catalyst can often be misleading [22]. Therefore, it is important to report the results in terms of photonic efficiency or formal quantum efficiency, which consider the irradiance and two dimensional area of catalyst. Very few researchers present photonic or formal quantum efficiency [23-27]. Nguyen et al. reported $1.86 \mu\text{mol h}^{-1} \text{g}^{-1}$ of methane and an overall quantum efficiency of 0.05% [28], and Collado and co-workers reported $0.4 \mu\text{mol h}^{-1} \text{g}^{-1}$ of methane but with an

apparent quantum efficiency of 2.7% [29]. The comparison of rates per gram of catalyst is not possible without considering the irradiance and the emission spectrum of the source. A similar comparison can be made between the work of Tseng et al. and Tahir et al. regarding methanol production [22, 30].

This study aims to evaluate the photocatalytic reduction of CO₂ in a gas phase batch reactor with well-defined reactor parameters, including the irradiance and emission spectrum of the source. A range of different photocatalytic materials were tested to determine differences in yield of products and their formal quantum efficiencies.

2. Materials and Methods

2.1. Catalyst Preparation

Three catalyst preparations were used in this study; unmodified TiO₂ (Evonik Aeroxide P25), Cu modified TiO₂ (P25) and TiO₂ nanotubes. Cu clusters, used for surface modification, were synthesized by adapting the Brust-Schiffrin protocol [31]. For the 1.0 wt% copper/titanium dioxide catalyst (denoted Cu-TiO₂), 1 wt% synthesized Cu clusters were mixed with TiO₂ (P25) by sonication in methanol followed by annealing at 550°C. TiO₂ nanotubes (denoted NT) were prepared by a hydrothermal method previously reported [32]. The catalyst powders were immobilised on borosilicate glass plates (25 mm x 20 mm) by spray coating until the desired weight was obtained (8 mg). The samples were then annealed at 450°C (Lenton furnace) in air for 2 h (ramp up 2°C min⁻¹ and ramp down 2°C min⁻¹).

2.2. Photocatalytic reactor

The gas phase stainless steel T-shaped reactor was composed of ultra-high vacuum (UHV) parts (Swagelok and Kurt J. Lesker) with an internal volume of 120 mL. The reactor was fitted with a quartz window to allow irradiation of the catalyst plates. The catalyst plates were placed inside the reactor facing the quartz window. A schematic of the reactor is given in figure 1. High purity water (Merck, SupraSolv 7732-18-5) was added to the reactor at the start of each experiment. A magnetic flea with stirrer was used to give mixing within the reactor. The temperature of the reactor was maintained with thermostatically controlled thermal tape at 70°C. The reactor was purged for 10 min with the feed gas mixture before sealing at a pressure of 2 bar. The feed gases for the reactor were CO₂ (BOC, UN1013, 99.99% purity) and Ar (BOC, UN1006, 99.998% purity).

The gaseous products obtained following irradiation was analysed by gas chromatography (GC) with a flame ionisation detector (FID) and using He (BOC, UN1046, 99.999% purity) as a carrier gas. The GC (Agilent Technologies, 7890B) was connected directly to the reactor outlet and samples were analysed every 30 min leading to a decrease in pressure inside the reactor (0.25 bar) each time a measurement was performed. Sampling from the reactor following the initial purge and fill cycle were denoted T₀, time zero with later samples denoted T₃₀, T₆₀ etc to detail the number of minutes elapsed from irradiation. The T₀ sample act as reference point for the purity and mixture of gasses present prior to initiation of reaction by irradiation. The reactor was purged and filled with a range of gas mixtures to provide conditions for CO₂ reduction, sample cleaning or absence of CO₂ control runs.

2.3. *CO₂ reduction*

A mixture of CO₂:Ar (20:80) was used to test CO₂ reduction in all experiments. This mixture was purged through the reactor prior to sealing the system at 2 bar with periodic sampling the gas mixture used to assess the generation of CO₂ reduction products. These tests were performed on fresh photocatalyst samples or following control runs, the conditions of which are detailed below.

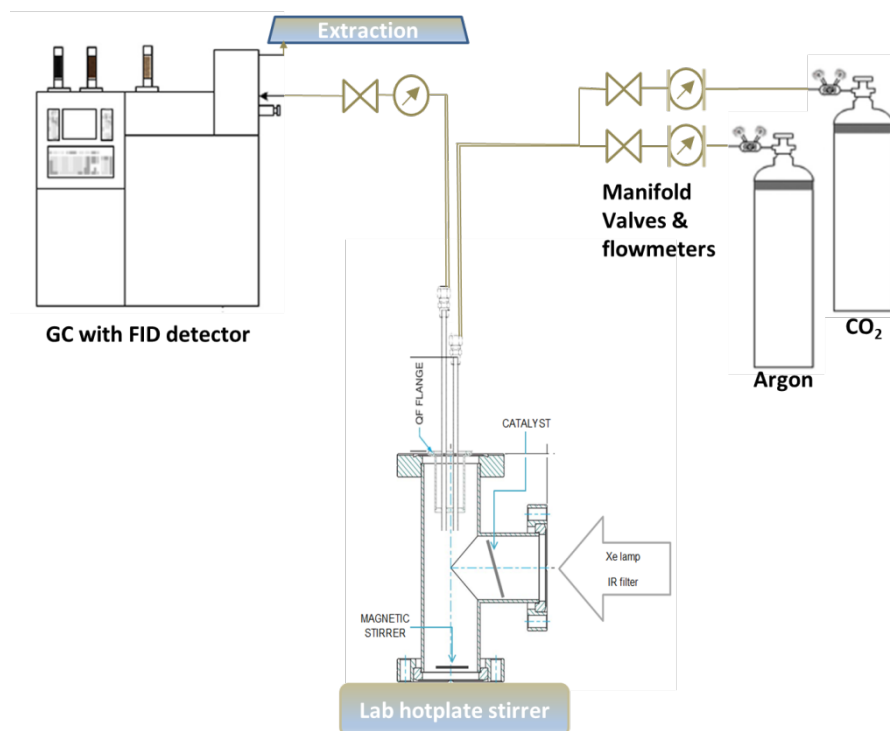


Fig. 1. Schematic diagram of the photocatalytic reaction apparatus

Control experiments in the absence of CO₂ were performed for each catalyst. For these experiments, the reactor conditions were the same as for CO₂ photoreduction; however, 100% Ar was used for the purging and filling the reactor, in the presence of 200 μ L of water. Due to the inverse relationship between gas solubility and temperature, experiments with hot water were performed to try to further eliminate CO₂ presence in the reactor for the control experiments. The procedure for each water condition added is detailed below:

- Cold water control: for all photocatalysts, room temperature deionised water was added to the reactor and it was heated after closing it.
- Hot water control: in this case, the water was heated to boiling before being added to the reactor that was already at 70°C. This process was carried out in control tests with P25 and NTs as photocatalysts.

2.4. *Irradiation source and formal quantum efficiency*

The photocatalytic reactor was irradiated with a Xe lamp (100 W, LOT Oriel) through a water IR filter. The spectral intensity incident on the reactor window was measured with a calibrated spectral radiometer consisting of Jobin Yvon Horiba Gemini 120 monochromator

and a SpectrAcq2 photomultiplier tube. The irradiance spectrum of the source is given in the supplementary information (Figure S1).

When using a polychromatic emission source the Formal Quantum Efficiencies (QE) should be reported [33]. The Formal Quantum efficiency is calculated using equation 1.

$$QE = \frac{\text{moles of electrons passed to form products}}{\text{moles of photons (250 – 410 nm, Einsteins)}} \quad (1)$$

It was assumed that wavelengths > 410 nm were not utilised by the photocatalytic materials based on previous photoelectrochemical studies determining the effective band gap [31].

3. Results and discussion

3.1. Photocatalytic reduction of CO₂

Photocatalysts materials were tested for the photocatalytic reduction of CO₂ using P25 as a bench mark reference. Controls in the absence of CO₂ were also performed for each photocatalyst. When using P25 as a photocatalyst, both CO and CH₄ products were observed with concentrations above the limit of detection (1.78 and 1.08 ppm respectively) after 4 h of irradiation (Fig 2 (a-b)). However, as it can be seen in figure 2 (a-b), similar concentrations were obtained when performing the controls in the absence of CO₂ in the feed gas (1.51 ppm for CO and 0.71 ppm for CH₄).

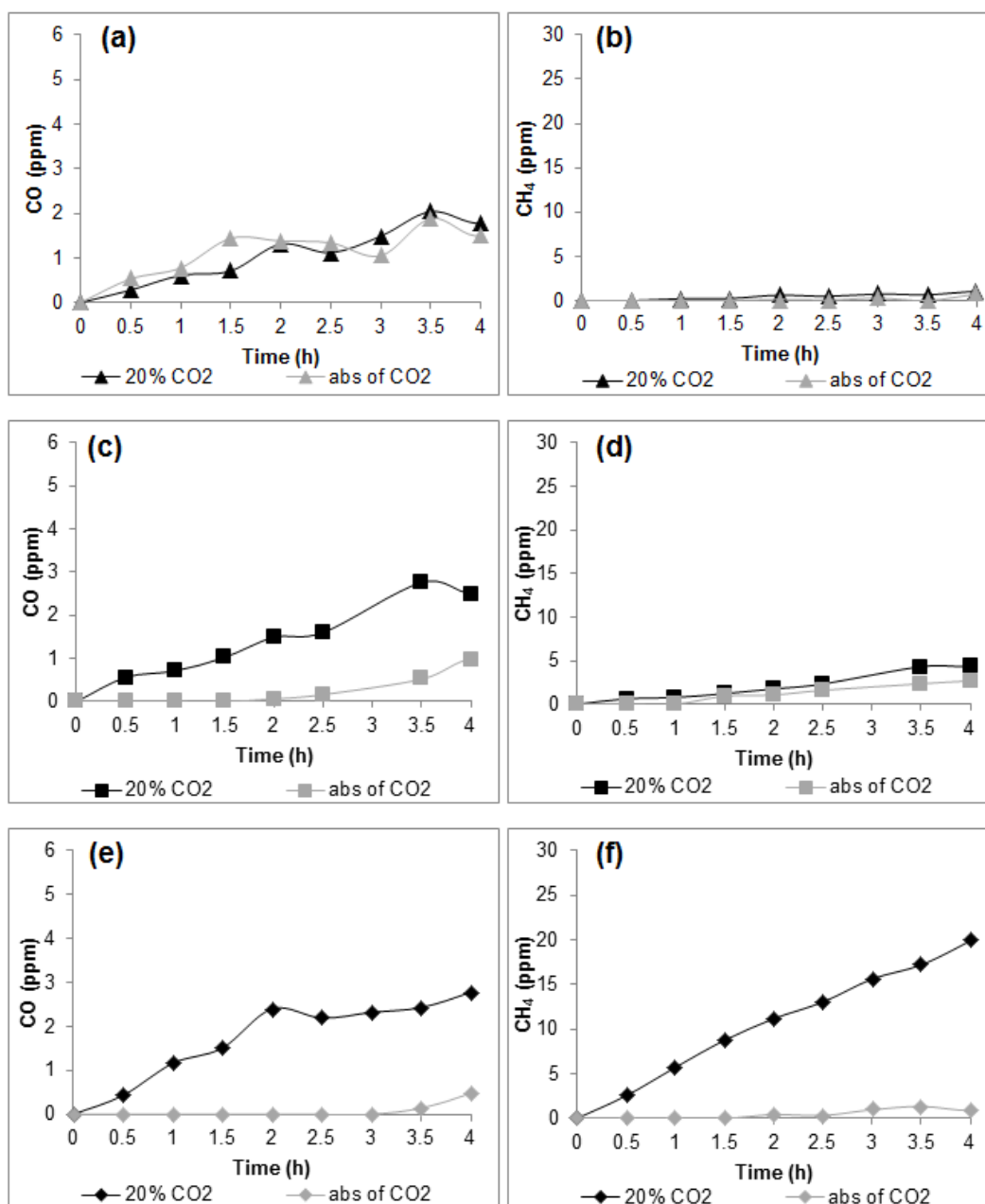


Fig. 2. CO and CH₄ production (in ppm) over time using different catalysts in the presence and absence of CO₂. (a-b) TiO₂ (P25), (c-d) Cu-TiO₂, (e-f) NT

Copper modified P25, previously investigated as a water splitting catalyst [31], was used under identical reactor conditions (fig. 2, (c-d)). We reported the physicochemical properties of the Cu-TiO₂ previously where the average size of the copper clusters was ~ 0.8-0.9 nm, which was measured with STEM (scanning transmission electron microscopy) at a spot size of 0.2 nm [31]. XPS analysis showed that the copper clusters were a mixture of Cu(0) and Cu(I) after loading onto the TiO₂ and annealing. In that work there was evidence of a small red shift in the effective band gap following Cu modification. Using incident photon to current conversion efficiency measurements, the effective band gap of unmodified P25 was 2.96 eV and for the Cu doped P25 the band gap was 2.85 eV equating to a small red-shift of 0.11 eV (16 nm). This small red shift may result in a small improvement in solar driven CO₂ reduction.

The Cu-TiO₂ was observed to yield higher concentrations of both products, CO and CH₄, (2.51 and 4.36 ppm, respectively) when compared to unmodified P25. The photocatalytic activity of Cu-TiO₂ was also tested in the absence of CO₂. For both CO and CH₄, the yields obtained in the absence of CO₂ were significantly lower than in the presence of CO₂ (CO = 0.96 ppm and CH₄ = 2.7 ppm).

TiO₂ nanotubes (NT) were also tested as photocatalysts for CO₂ photoreduction (fig. 2 (e-f)). The NT were produced by a hydrothermal method previously reported [32] which gave tubes with an inner diameter between 4-6 nm and an outer diameter between 8-12 nm respectively. In that work, XRD analysis showed that the tubes were predominantly anatase TiO₂. Tubes annealed at 400°C were mesoporous with pore sizes between 2 and 50 nm, where a pore size less than 10 nm corresponded to the inner diameter of the nanotubes and the larger pores (10-100 nm) were attributed to the aggregation of the nanotubes.

In terms of CO production, the results were similar to the ones obtained with Cu-TiO₂ (2.78 ppm). The NTs proved to be more efficient for CH₄ production than the other two photocatalysts tested, obtaining a concentration of 19.89 ppm after 4 h of irradiation. When the control experiments were performed in the absence of CO₂, the CO and CH₄ concentrations yielded were much lower than in the presence of CO₂ (0.48 ppm for CO and 0.87 ppm for CH₄). The presence of small quantities of CO₂ reduction products in the absence of CO₂ in the gas feed prompted an investigation into sources of trace CO₂ in the reactor.

3.2. Additional controls in the absence of CO₂

Calculation of CO₂ peak areas in GC at T₀ for CO₂ control measurements showed a very low concentration of CO₂ to be present, in the ~10-20 μMol range. A calculation of the amount of CO₂ potentially dissolved in the feed water added to the reactor yielded a value ~8 μMol as a possible source for the concentrations observed in GC analysis of T₀ samples. Control experiments in the absence of CO₂ in the feed gas were repeated where the feed water was pre-boiled to remove dissolved CO₂. With pre-boiled feed water, the peak area for CO₂ at T₀ was half that observed with non-treated water (12.5 and 4.4 μMol respectively).

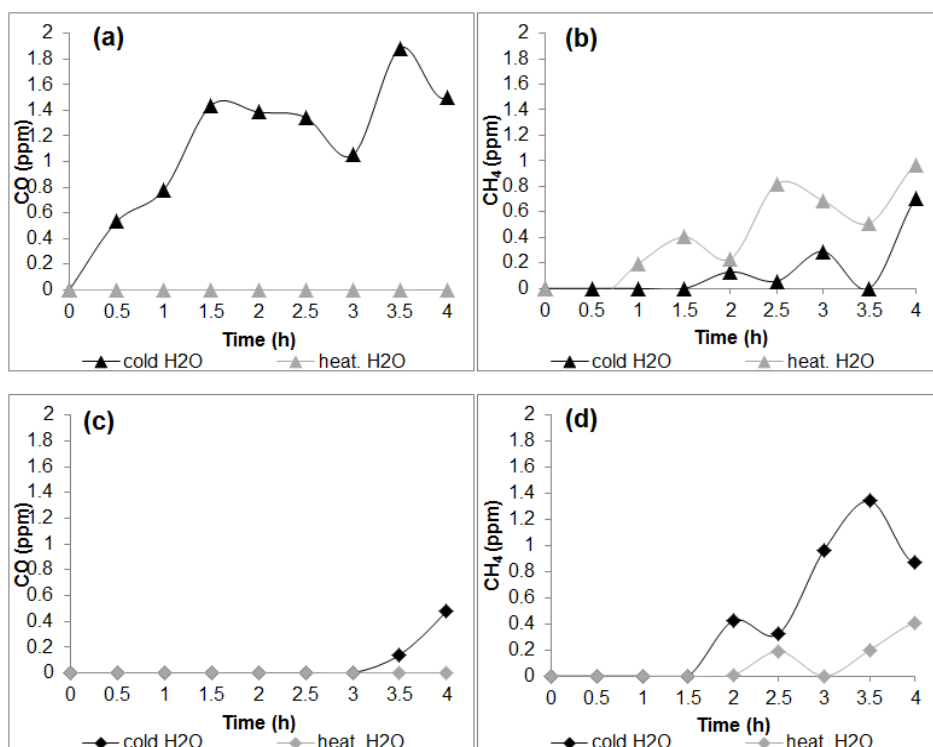


Fig. 3. CO and CH₄ production (in ppm) over time in the controls in the absence of CO₂ performed with addition of cold or of heated water. (a-b) P25, (c-d) NT

With small quantities of CO₂ still being present in hot water, the control in the absence of CO₂ in the feed gas gave much smaller amounts of CO and CH₄ (see fig 3). With the P25 control (fig. 3. (a-b)), both the hot water and the cold water concentrations for CH₄ production were below or close to the detection limit (0.75 ppm) and cannot be considered as significant. For the NT samples, the CH₄ concentrations obtained with cold water added are above the limit of detection after 3 h of irradiation but with heated water the CH₄ produced is below the detection limit. For the NTs and cold water, CO production is observed above the detection limit (1.58 ppm) after 3.5 h of irradiation but with heated water the CO production is below the detection limit. Some authors have suggested that a pre-cleaning step is necessary to ensure the adsorption sites, and therefore potential active sites, are not occupied [34, 35].

When performing the control experiments in the absence of CO₂ in the feed gas, with NTs as the photocatalyst, adding pre-boiled water resulted in a lower initial concentration of CO₂ of 6.7 μ Mol at T₀ when compared with control with non pre-boiled water (18.2 μ Mol at T₀).

It is difficult to remove all CO₂ from the reactor. Although using pre-boiled feed water reduced the detected CO₂ at T₀, a small but still detectable peak for CO₂ remained. The source of this CO₂ is not immediately obvious as the reactor was purged with argon (99.998% purity, possibly 20 ppm unknown) and the water degassed. Due to equilibrium with CO₂ in the atmosphere, CO₂ as bicarbonate monolayer coverage have previously been observed [21]. We have observed changes to carbonate type, bicarbonate carbonate equilibrium, under differing surface treatments and photocatalytic conditions [35-37]. Previous studies on carbonates as a source of CO₂ reduction products have argued that

decomposition of carbonates are more likely to lead to CO₂ rather than reduced products [35]. Decomposition of surface carbonates may yield CO₂. Indeed, if the surface of the catalyst is contaminated with low levels of organic carbon impurities, photocatalytic oxidation of these compounds would release CO₂.

3.3. Yields and Formal Quantum Efficiency

To compare the product yields obtained in this study with those of other researchers, caution should be taken as the yields obtained can be heavily influenced by reactor geometry and conditions employed. In this regard, the comparative yields given in table 1 were made with reported reactors using the same volume and type of light source to minimise the influence of reaction conditions. However, even when comparing similar reactors and conditions, many researchers normalise their results to a yield per gram of photocatalyst, which can be misleading, biasing the result towards reactors that utilise smaller amounts of catalyst e.g. thin films. This comparison is even more complicated when no data is provided to show whether product yields scale linearly with catalyst loading (and the assumption that the product yield will increase upon increasing photocatalyst loading may not be easily engineered to maintain the same irradiated photocatalyst area or mass). In addition, this normalised photocatalytic reaction rate is often measured as an average over a number of hours, despite the reaction kinetics changing over this time period for some materials.

The yields reported by others cannot be directly compared as there are differences in reactor systems, although the yields reported by others in terms of $\mu\text{mol h}^{-1} \text{g}^{-1}_{\text{cat}}$ are within one order of magnitude to those observed in this work (Table 1). Zhai et al. [38], reported higher yields of CO and CH₄ for both P25 and Cu-TiO₂, however they used a 200 W Xe source whereas in this work we used a 100 W Xe source. Zhai et al. did not report the light intensity entering the reactor or the area of catalyst irradiated, nor do they calculate formal quantum yield. The irradiance will be a dominant factor controlling the yield [39]. Gonell et al. [40] reported a range of yields for CO and CH₄ using Cu-TiO₂ in a water based solvent system with and without electron donor. In the presence of electron donor, they observed the highest yield of CO, no CH₄ and increased yields for H₂. The use of different reactor systems and different irradiance sources means that direct comparison of results is impossible and strongly supports the need for standardised systems or conditions for comparison of results for photocatalytic CO₂ reduction.

The reporting of Photonic Efficiency (Apparent Quantum Yield) for monochromatic sources, or Formal Quantum Efficiency (FQE) for polychromatic sources, is more appropriate for correlation of results from different groups. In the present work the FQE for each photocatalyst were calculated according to equation 1 (the irradiance of the source is given in figure S1) and are given in table 1.

Table 1: Product yields after 4 h of irradiation and formal quantum efficiency (Q.E) obtained in this work vs yields and quantum efficiency observed in the literature (under comparable reactor conditions)

Catalyst	Ref. Yields ($\mu\text{mol h}^{-1} \text{g}^{-1} \text{cat}$)		Ref.	Yields obtained in this work ($\mu\text{mol h}^{-1} \text{g}^{-1} \text{cat}$)		Formal Q.E (250 - 410 nm)		
	CO	CH ₄		CO	CH ₄	CO	CH ₄	CO ₂
P25	1.2	0.38	[41]	0.41	0.25	1.29×10^{-5}	3.12×10^{-5}	4.41×10^{-5}
P25	2.5	1.2	[38]					
Cu-TiO ₂	5.4	8.7	[40]	0.58	1.01	1.82×10^{-5}	1.26×10^{-4}	1.44×10^{-4}
	0.3 - 2.8*	0 - 0.3*						
NT	-	1.48	[32]	0.64	4.61	2.01×10^{-5}	5.75×10^{-4}	5.95×10^{-4}

^aGonell et al [40] report a range of values for CO and CH₄ yield in a liquid phase reactor with different solvents and with/without electron donor. With electron donor no CH₄ was produced and increased yields CO and H₂ were observed.

As it can be seen in table 1, the calculated FQE obtained for CO and CH₄ products are very low, as are the overall FQE for CO₂ reduction. The order of efficiency for CO, CH₄ production and overall CO₂ reduction was NT>Cu-TiO₂>P25. The modification of the P25 with Cu clusters (mixed oxidation state of Cu (0) and Cu (1)) gives a slight red shift in the effective band gap as previously reported [31]. Cu₂O has a more negative conduction band edge than TiO₂ (anatase or rutile) and this may lead to the slight improvement in the efficiency for CO₂ reduction as compared to the unmodified P25 unmodified. Hori (2008) reported that for the electrochemical reduction of CO₂, copper had a higher affinity to produce hydrocarbons, when compared to other metals [42], but was also able to produce CO. The major difference in the efficiency of the materials observed in this work was the enhanced yield of CH₄ observed with the TiO₂ NTs as compared to Cu-TiO₂ and P25. In previous work it was reported that enhanced efficiency for CO₂ reduction on NTs was due to a high concentration of undercoordinated titanium sites, which was supported by EPR analysis [32].

The quantum efficiency of photocatalytic CO₂ reduction is rarely reported. However, in the cases it has been calculated, the efficiency is typically very low [43-45]. To understand the typically low efficiencies observed during photocatalytic CO₂ reduction the current understanding of the mechanism by which CO₂ generates these products and alternative back or side reactions should be considered. There are a number of CO₂ pathways named after key intermediates, formaldehyde [46, 47], carbene [48] and glyoxal pathways [18, 35], reported to explain the steps in CO₂ reduction to the commonly observed products, methane, methanol, carbon monoxide etc. All of these pathways assumes the single electron reduction of CO₂ to CO₂^{•-}, although this reaction is high energy step requiring a very negative electrochemical potential [35] which is either too negative to be achieved with the conduction band of most of the photocatalysts reported or, if achievable, leaves limited overpotential to drive this reaction. All of these potential mechanisms have been investigated under ultra-pure conditions [18, 35, 49] and none of the mechanisms were considered to be representative of all the steps occurring in photocatalytic CO₂ reduction. However these reports did show that the glyoxal pathway may occur, but is likely a minor path, with an alternative undiscovered pathway leading to acetaldehyde postulated [35]. One interesting aspect of the glyoxal pathway and the alternative path through acetaldehyde differing from the carbene or formaldehyde pathways is both of these newer pathways require

intermediates that are generated by oxidation reactions. If the glyoxal pathway or a newer pathway incorporating some of its steps is shown to be the correct mechanism, by which photocatalytic CO₂ reduction occurs, then low efficiency reported may be an artefact due to incorrectly addressing the number of electrons required to reduce CO₂. One aspect considered in glyoxal pathway that may also explain the low efficiencies reported is the degree of back reaction i.e., re-oxidation of reduced CO₂ products by valence band holes. A recent study to this effect observed that photocatalysts that were good at degrading ethane, ethylene or methane were poor reducing CO₂, whereas photocatalysts that were modified to reduce the efficiency for oxidising these compounds showed improved yields of these CO₂ reduction products suggesting that blocking re-oxidation of products may be a route to improving activity for CO₂ reduction [50]. Considering that re-oxidation of CO₂ reduction products and intermediates has been observed, these back reactions may explain the low efficiencies often observed in photocatalytic CO₂ reduction.

4. Conclusions

Improvement in the activity for photocatalytic reduction of CO₂ was observed following surface modification using Cu clusters, or nanoengineering of the titania to give nanotubes. These modification strategies studied, showed increases in yields consistent with previous reports in the literature. The order of efficiency for CO, CH₄ production and overall CO₂ reduction was NT>Cu-TiO₂>P25. Formal Quantum Efficiencies were determined for the photocatalytic reduction of CO₂ and showed that even where reasonable product yields were observed, as compared to literature, the FQE were very low. Of the photocatalysts tested in this study, the nanotubes prepared using a hydrothermal route, showed a marked improvement in CH₄ production as compared to the Cu-TiO₂ and the unmodified P25.

5. Acknowledgements

We wish to acknowledge funding from the US-Ireland R&D Collaborative Partnership Program NSF (CBET-1438721), SFI (SFI 14/US/E2915) and DfE (USI065) and the financial support from British Council under the STREAM-MENA Institutional Links Scheme (Grant number 278072873).

6. References:

- [1] O. Ola, M.M. Maroto-Valer, Review of material design and reactor engineering on TiO₂ photocatalysis for CO₂ reduction, *Journal of Photochemistry and Photobiology C: Photochemistry Reviews*, 24 (2015) 16-42.
- [2] K. Li, X. An, K.H. Park, M. Khraisheh, J. Tang, A critical review of CO₂ photoconversion: Catalysts and reactors, *Catalysis Today*, 224 (2014) 3-12.
- [3] P. Akhter, M. Hussain, G. Saracco, N. Russo, Novel nanostructured-TiO₂ materials for the photocatalytic reduction of CO₂ greenhouse gas to hydrocarbons and syngas, 2015.
- [4] C. Finn, S. Schnittger, L.J. Yellowlees, J.B. Love, Molecular approaches to the electrochemical reduction of carbon dioxide, *Chemical Communications*, 48 (2012) 1392-1399.
- [5] J.L. White, M.F. Baruch, J.E. Pander lii, Y. Hu, I.C. Fortmeyer, J.E. Park, T. Zhang, K. Liao, J. Gu, Y. Yan, T.W. Shaw, E. Abelev, A.B. Bocarsly, Light-Driven Heterogeneous

- Reduction of Carbon Dioxide: Photocatalysts and Photoelectrodes, *Chemical Reviews*, 115 (2015) 12888-12935.
- [6] M. Pelaez, N.T. Nolan, S.C. Pillai, M.K. Seery, P. Falaras, A.G. Kontos, P.S.M. Dunlop, J.W.J. Hamilton, J.A. Byrne, K. O'Shea, M.H. Entezari, D.D. Dionysiou, A review on the visible light active titanium dioxide photocatalysts for environmental applications, *Applied Catalysis B: Environmental*, 125 (2012) 331-349.
- [7] T. Yui, A. Kan, C. Saitoh, K. Koike, T. Ibusuki, O. Ishitani, Photochemical Reduction of CO₂ Using TiO₂: Effects of Organic Adsorbates on TiO₂ and Deposition of Pd onto TiO₂, *ACS Applied Materials & Interfaces*, 3 (2011) 2594-2600.
- [8] K. Iizuka, T. Wato, Y. Miseki, K. Saito, A. Kudo, Photocatalytic Reduction of Carbon Dioxide over Ag Cocatalyst-Loaded Al_{0.4}Ti₄O₁₅ (A = Ca, Sr, and Ba) Using Water as a Reducing Reagent, *Journal of the American Chemical Society*, 133 (2011) 20863-20868.
- [9] Q. Kang, T. Wang, P. Li, L. Liu, K. Chang, M. Li, J. Ye, Photocatalytic Reduction of Carbon Dioxide by Hydrous Hydrazine over Au–Cu Alloy Nanoparticles Supported on SrTiO₃/TiO₂ Coaxial Nanotube Arrays, *Angewandte Chemie International Edition*, 54 (2015) 841-845.
- [10] Y.-X. Pan, Z.-Q. Sun, H.-P. Cong, Y.-L. Men, S. Xin, J. Song, S.-H. Yu, Photocatalytic CO₂ reduction highly enhanced by oxygen vacancies on Pt-nanoparticle-dispersed gallium oxide, *Nano Research*, 9 (2016) 1689-1700.
- [11] F. Sastre, A.V. Puga, L. Liu, A. Corma, H. García, Complete Photocatalytic Reduction of CO₂ to Methane by H₂ under Solar Light Irradiation, *Journal of the American Chemical Society*, 136 (2014) 6798-6801.
- [12] K. Teramura, S. Iguchi, Y. Mizuno, T. Shishido, T. Tanaka, Photocatalytic Conversion of CO₂ in Water over Layered Double Hydroxides, *Angewandte Chemie*, 124 (2012) 8132-8135.
- [13] C.-C. Yang, Y.-H. Yu, B. van der Linden, J.C.S. Wu, G. Mul, Artificial Photosynthesis over Crystalline TiO₂-Based Catalysts: Fact or Fiction?, *Journal of the American Chemical Society*, 132 (2010) 8398-8406.
- [14] B. Alotaibi, X. Kong, S. Vanka, S.Y. Woo, A. Pofelski, F. Oudjedi, S. Fan, M.G. Kibria, G.A. Botton, W. Ji, H. Guo, Z. Mi, Photochemical Carbon Dioxide Reduction on Mg-Doped Ga(In)N Nanowire Arrays under Visible Light Irradiation, *ACS Energy Letters*, 1 (2016) 246-252.
- [15] H.-C. Hsu, I. Shown, H.-Y. Wei, Y.-C. Chang, H.-Y. Du, Y.-G. Lin, C.-A. Tseng, C.-H. Wang, L.-C. Chen, Y.-C. Lin, K.-H. Chen, Graphene oxide as a promising photocatalyst for CO₂ to methanol conversion, *Nanoscale*, 5 (2013) 262-268.
- [16] S. Iguchi, K. Teramura, S. Hosokawa, T. Tanaka, Photocatalytic conversion of CO₂ in an aqueous solution using various kinds of layered double hydroxides, *Catalysis Today*, 251 (2015) 140-144.
- [17] S. Wang, X. Wang, Photocatalytic CO₂ reduction by CdS promoted with a zeolitic imidazolate framework, *Applied Catalysis B: Environmental*, 162 (2015) 494-500.
- [18] I.A. Shkrob, T.W. Marin, H. He, P. Zapol, Photoredox Reactions and the Catalytic Cycle for Carbon Dioxide Fixation and Methanogenesis on Metal Oxides, *The Journal of Physical Chemistry C*, 116 (2012) 9450-9460.
- [19] W. Chanmanee, M.F. Islam, B.H. Dennis, F.M. MacDonnell, Solar photothermochemical alkane reverse combustion, *Proceedings of the National Academy of Sciences*, 113 (2016) 2579.
- [20] Retraction for Chanmanee et al., Solar photothermochemical alkane reverse combustion, *Proceedings of the National Academy of Sciences*, 115 (2018) E557.
- [21] A. Song, E.S. Skibinski, W.J.I. DeBenedetti, A.G. Ortoll-Bloch, M.A. Hines, Nanoscale Solvation Leads to Spontaneous Formation of a Bicarbonate Monolayer on Rutile (110) under Ambient Conditions: Implications for CO₂ Photoreduction, *The Journal of Physical Chemistry C*, 120 (2016) 9326-9333.
- [22] I.H. Tseng, W.-C. Chang, J.C.S. Wu, Photoreduction of CO₂ using sol–gel derived titania and titania-supported copper catalysts, *Applied Catalysis B: Environmental*, 37 (2002) 37-48.

- [23] W.-N. Wang, W.-J. An, B. Ramalingam, S. Mukherjee, D.M. Niedzwiedzki, S. Gangopadhyay, P. Biswas, Size and Structure Matter: Enhanced CO₂ Photoreduction Efficiency by Size-Resolved Ultrafine Pt Nanoparticles on TiO₂ Single Crystals, *Journal of the American Chemical Society*, 134 (2012) 11276-11281.
- [24] J.C.S. Wu, T.-H. Wu, T. Chu, H. Huang, D. Tsai, Application of Optical-fiber Photoreactor for CO₂ Photocatalytic Reduction, *Topics in Catalysis*, 47 (2008) 131-136.
- [25] P.-Y. Liou, S.-C. Chen, J.C.S. Wu, D. Liu, S. Mackintosh, M. Maroto-Valer, R. Linforth, Photocatalytic CO₂ reduction using an internally illuminated monolith photoreactor, *Energy & Environmental Science*, 4 (2011) 1487-1494.
- [26] O. Ola, M. Maroto-Valer, D. Liu, S. Mackintosh, C.-W. Lee, J.C.S. Wu, Performance comparison of CO₂ conversion in slurry and monolith photoreactors using Pd and Rh-TiO₂ catalyst under ultraviolet irradiation, *Applied Catalysis B: Environmental*, 126 (2012) 172-179.
- [27] W.-H. Lee, C.-H. Liao, M.-F. Tsai, C.-W. Huang, J.C.S. Wu, A novel twin reactor for CO₂ photoreduction to mimic artificial photosynthesis, *Applied Catalysis B: Environmental*, 132-133 (2013) 445-451.
- [28] T.-V. Nguyen, J.C.S. Wu, Photoreduction of CO₂ to fuels under sunlight using optical-fiber reactor, *Solar Energy Materials and Solar Cells*, 92 (2008) 864-872.
- [29] L. Collado, P. Jana, B. Sierra, J.M. Coronado, P. Pizarro, D.P. Serrano, V.A. de la Peña O'Shea, Enhancement of hydrocarbon production via artificial photosynthesis due to synergetic effect of Ag supported on TiO₂ and ZnO semiconductors, *Chemical Engineering Journal*, 224 (2013) 128-135.
- [30] M. Tahir, N.S. Amin, Photocatalytic CO₂ reduction and kinetic study over In/TiO₂ nanoparticles supported microchannel monolith photoreactor, *Applied Catalysis A: General*, 467 (2013) 483-496.
- [31] P.K. Sharma, M.A.L.R.M. Cortes, J.W.J. Hamilton, Y. Han, J.A. Byrne, M. Nolan, Surface modification of TiO₂ with copper clusters for band gap narrowing, *Catalysis Today*, (2017).
- [32] B. Vijayan, N.M. Dimitrijevic, T. Rajh, K. Gray, Effect of Calcination Temperature on the Photocatalytic Reduction and Oxidation Processes of Hydrothermally Synthesized Titania Nanotubes, *The Journal of Physical Chemistry C*, 114 (2010) 12994-13002.
- [33] A. Mills, S. Le Hunte, An overview of semiconductor photocatalysis, *Journal of Photochemistry and Photobiology A: Chemistry*, 108 (1997) 1-35.
- [34] M. Dilla, A. Mateblowski, S. Ristig, J. Strunk, Photocatalytic CO₂ Reduction under Continuous Flow High-Purity Conditions: Influence of Light Intensity and H₂O Concentration, *ChemCatChem*, 9 (2017) 4345-4352.
- [35] A. Pougin, M. Dilla, J. Strunk, Identification and exclusion of intermediates of photocatalytic CO₂ reduction on TiO₂ under conditions of highest purity, *Physical Chemistry Chemical Physics*, 18 (2016) 10809-10817.
- [36] K.C. Schwartzenberg, J.W.J. Hamilton, A.K. Lucid, E. Weitz, J. Notestein, M. Nolan, J.A. Byrne, K.A. Gray, Multifunctional photo/thermal catalysts for the reduction of carbon dioxide, *Catalysis Today*, 280 (2017) 65-73.
- [37] K. Schwartzenberg, The Synthesis and Characterization of Multifunctional Titania-based Materials for the Photo/Thermal Catalytic Reduction of CO₂, *Civil and Environmental Engineering, Northwestern University, ProQuest Dissertations And Theses; Thesis (Ph.D.)--Northwestern University*, 2015, pp. 1-166.
- [38] Q. Zhai, S. Xie, W. Fan, Q. Zhang, Y. Wang, W. Deng, Y. Wang, Photocatalytic conversion of carbon dioxide with water into methane: platinum and copper (I) oxide co-catalysts with a core-shell structure, *Angewandte Chemie*, 125 (2013) 5888-5891.
- [39] K. Kočí, L. Obalová, Z. Lacný, Photocatalytic reduction of CO₂ over TiO₂ based catalysts, *Chemical Papers*, 62 (2008) 1-9.
- [40] F. Gonell, A.V. Puga, B. Julián-López, H. García, A. Corma, Copper-doped titania photocatalysts for simultaneous reduction of CO₂ and production of H₂ from aqueous sulfide, *Applied Catalysis B: Environmental*, 180 (2016) 263-270.

- [41] S. Xie, Y. Wang, Q. Zhang, W. Deng, Y. Wang, MgO- and Pt-Promoted TiO₂ as an Efficient Photocatalyst for the Preferential Reduction of Carbon Dioxide in the Presence of Water, *ACS Catalysis*, 4 (2014) 3644-3653.
- [42] Y.i. Hori, Electrochemical CO₂ reduction on metal electrodes, *Modern aspects of electrochemistry*, Springer2008, pp. 89-189.
- [43] M. Tahir, N.S. Amin, Performance analysis of nanostructured NiO–In₂O₃/TiO₂ catalyst for CO₂ photoreduction with H₂ in a monolith photoreactor, *Chemical Engineering Journal*, 285 (2016) 635-649.
- [44] B.-J. Liu, T. Torimoto, H. Yoneyama, Photocatalytic reduction of carbon dioxide in the presence of nitrate using TiO₂ nanocrystal photocatalyst embedded in SiO₂ matrices, *Journal of Photochemistry and Photobiology A: Chemistry*, 115 (1998) 227-230.
- [45] Y. Li, W.-N. Wang, Z. Zhan, M.-H. Woo, C.-Y. Wu, P. Biswas, Photocatalytic reduction of CO₂ with H₂O on mesoporous silica supported Cu/TiO₂ catalysts, *Applied Catalysis B: Environmental*, 100 (2010) 386-392.
- [46] M. Subrahmanyam, S. Kaneco, N. Alonso-Vante, A screening for the photo reduction of carbon dioxide supported on metal oxide catalysts for C₁–C₃ selectivity, *Applied Catalysis B: Environmental*, 23 (1999) 169-174.
- [47] N. Sasirekha, S.J.S. Basha, K. Shanthi, Photocatalytic performance of Ru doped anatase mounted on silica for reduction of carbon dioxide, *Applied Catalysis B: Environmental*, 62 (2006) 169-180.
- [48] M. Anpo, H. Yamashita, Y. Ichihashi, S. Ehara, Photocatalytic reduction of CO₂ with H₂O on various titanium oxide catalysts, *Journal of Electroanalytical Chemistry*, 396 (1995) 21-26.
- [49] I.A. Shkrob, N.M. Dimitrijevic, T.W. Marin, H. He, P. Zapol, Heteroatom-Transfer Coupled Photoreduction and Carbon Dioxide Fixation on Metal Oxides, *The Journal of Physical Chemistry C*, 116 (2012) 9461-9471.
- [50] M.S. Hamdy, R. Amrollahi, I. Sinev, B. Mei, G. Mul, Strategies to Design Efficient Silica-Supported Photocatalysts for Reduction of CO₂, *Journal of the American Chemical Society*, 136 (2014) 594-597.

Supplementary Information

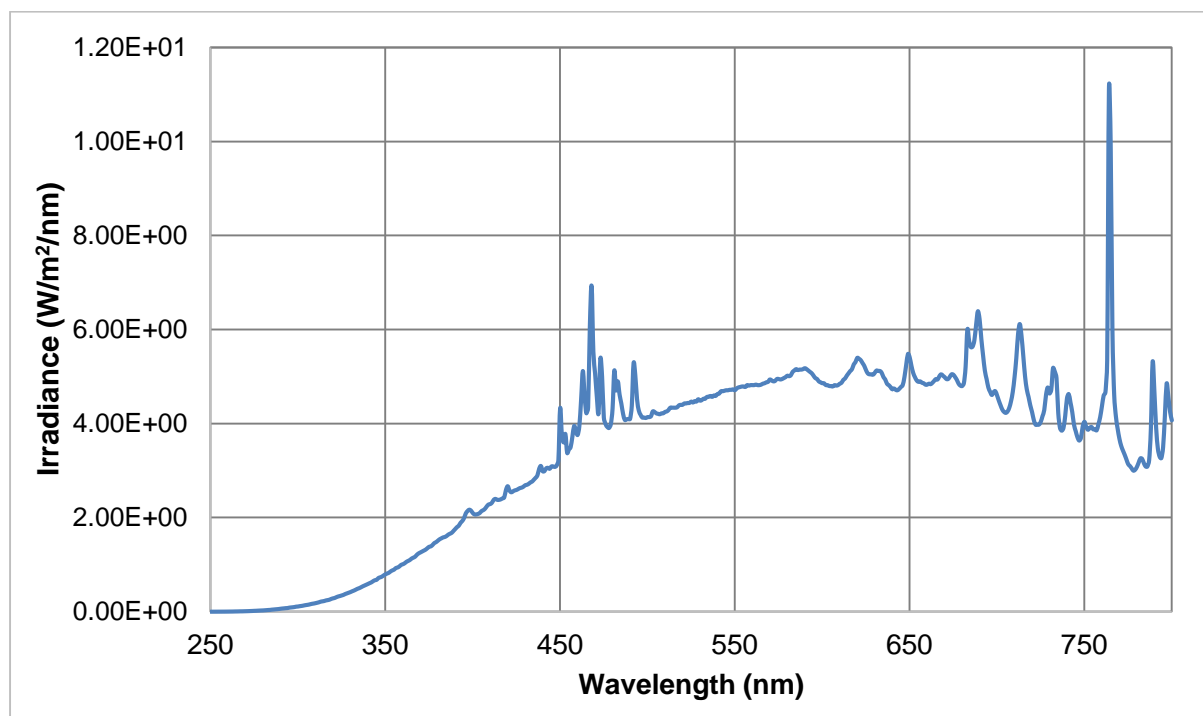


Figure S1 - Measured irradiance from 125W Xe lamp with IR filter